Geophysical Research Letters

RESEARCH LETTER
10.1029/2020GL087825

Sinking Versus Suspended Particle Size Distributions in the North Pacific Subtropical Gyre

B. B. Cael[1,2] and Angelicque E. White[2]

[1]National Oceanography Centre, Southampton, UK, [2]Center for Microbial Research and Education, University of Hawai'i at Manoa, Honolulu, HI, USA

Key Points:
- Comparing sinking and suspended particle size spectra implies an approximately linear diameter-sinking speed relationship at Station ALOHA
- This implies particles are fractal with $D \approx 2$, consistent with observations of marine aggregates
- Use of many sediment trap replicates ($n = 11$–12) over two deployments and multiple estimates of particle size increase confidence in this scaling

Correspondence to:
B. B. Cael,
cael@noc.ac.uk

Citation:
Cael, B. B., & White, A. E. (2020). Sinking versus suspended particle size distributions in the North Pacific Subtropical Gyre. *Geophysical Research Letters*, *47*, e2020GL087825. https://doi.org/10.1029/2020GL087825

Received 6 MAR 2020
Accepted 3 MAY 2020
Accepted article online 8 JUL 2020

Abstract The particle size distribution (PSD) is a fundamental property that influences all aspects of phytoplankton ecology. In particular, the size (e.g., diameter d [μm]) and sinking speed w (m/day) of individual particles are inextricable, but much remains unknown about how d and w are related quantitatively for bulk particulate matter. There is significant interest in inferring sinking mass fluxes from PSDs, but doing so requires knowing how both mass and w scale with d. To this end, using both laser diffraction and imaging, we characterized for the first time both sinking and suspended PSDs in the oligotrophic North Pacific subtropical gyre. Comparing these PSDs via a power law parameterization indicates an approximately linear w-to-d scaling, suggesting particles are more fractal-like than sphere-like in this respect. This result is robust across multiple instruments, depths, and sediment trap deployments and is made comparatively precise by a high degree of replication.

Plain Language Summary Particles are the embodiment of life in the ocean. They are unicellular, multicellular, aggregated, disaggregated, alive, and dead. The sinking and transport of particles out of the well-lit surface into the darkened depths serve to move mass and energy, thus connecting the entire ocean microbiome and profoundly influencing global elemental cycles. How fast particles sink is key to this transport and is to first-order dependent on particle size—but how size and sinking speed are related for complex assemblages of particles can be difficult to discern outside of controlled laboratory settings. We inferred a size-sinking relationship by comparing the size distributions of particles in the water column with those of sinking particles collected in sediment traps in the North Pacific Subtropical Gyre. Sinking speeds robustly appear to increase ~ linearly with particle diameter. This relationship is consistent with observations of the fractal structure of marine aggregates and has important implications for methods that estimate particle-mediated transport from water column particle-size distribution data.

1. Introduction

Among the many ecosystem services provided by the global ocean, sequestration of organic matter via the biological pump is one of the most critical to setting the elemental composition of the coupled ocean-atmosphere system. Understanding this complex process has been a central focus in biological and chemical oceanography since the 1970s (Berger, 1971; Honjo et al., 1980), when coordinated efforts were begun to characterize the time-varying vertical flux of mass and elements from the surface to the deep sea. As particles sink, they are rapidly respired, solubilized, and disaggregated (Collins et al., 2015), with less than ~15% of the primary production produced in the euphotic zone being exported in oligotrophic open ocean regimes (Karl et al., 2012). The fundamental balance is between the speed at which particles sink and the rate at which the material they comprise is returned to the ambient surroundings; the faster the sinking speed relative to these flux-attenuating processes, the deeper the resulting vertical mass transport, and by and large the longer the sequestration of transported material from the atmosphere (DeVries et al., 2012).

Particles' sinking speeds (w, [m/day]) are therefore a critical facet of the biological pump. Particles' sinking speeds vary by orders of magnitude in the ocean; particles sinking from only a few meters per day to kilometers per day all can contribute appreciably to the total flux (Trull et al., 2008). Therefore, it is essential to consider the *distribution* of sinking speeds. Size is a key determinant of the interaction between particles and their fluid environment, making size (here we define this in terms of diameter d [m]) and sinking speed inextricable (Smayda, 1970). This suggests a fundamental connection between the distribution of w and the particle size distribution (PSD)—itself the object of intense study in marine ecology and biogeochemistry,

strongly tied to community structure and function (Chisholm, 1992; White et al., 2015). Variations in other particle properties such as density (Kundu et al., 2012), porosity (Alldredge & Gotschalk, 1988), shape (Jackson, 1995), and (dis)aggregation (Burd & Jackson, 2009) influence their sinking speeds and complicate this relationship for individual particles (Jouandet et al., 2011; Laurenceau-Cornec et al., 2015), such that w and d do not exhibit a simple or exact relationship; rather, any relationship between these quantities can only be in a weak or statistical sense. While size is an imperfect variable for understanding sinking speeds, it is still plausible that, over a large collection of particles, size and sinking speed are quantitatively related, that is, that the distribution of w is predictably related to the PSD.

Though imperfect in their collection efficiency (Buesseler et al., 2007; Gardner, 2000), sediment traps—the "rain gauges" of ocean biogeochemistry—are the most broadly utilized means to collect sinking particles in situ for determination of size, elemental composition, and identity of passively sinking particulate matter. It is widely acknowledged that the measurement of sinking fluxes is a challenging endeavor involving many potential sources of error—especially in oligotrophic environments where signals tend to be small even while properties of interest can be surprisingly variable. Alternative methods for estimating sinking particle fluxes therefore have tremendous appeal, as do visualization and optical approaches that can validate at least qualitatively the basic assumptions underlying the concept of the biological pump, as was the initial impetus for polyacrylamide gel traps (McDonnell & Buesseler, 2010). Another such method that has become increasingly prevalent in the past several years, and will become increasingly essential for studying the biological pump as integrated optical sensor packages become more widely used, is based on the Underwater Vision Profiler (UVP) (Guidi et al., 2008). The UVP images the ambient PSD in the water column and then estimates a flux $\mathscr{F}$ according to (Guidi et al., 2008)

$$\mathscr{F} = \int_0^\infty n(d)m(d)w(d)\ \mathrm{d}d, \tag{1}$$

where $n(d)$ is the unnormalized PSD, $m(d)$ is the average mass (or moles of a given element) for particles of diameter d, and $w(d)$ is the mean sinking speed for particles of diameter d. $n(d)$ we refer to as the *suspended* PSD, that is, the PSD of all particles in the ambient fluid environment; multiplying $n(d)$ by $w(d)$ then yields the *sinking* PSD (here we define $s(d) = n(d)w(d)$); the mass each particle carries with it as it sinks, that is, $m(d)$, then yields the mass flux. Here the total flux is determined ultimately by the distribution of w and particles' masses, both as inferred from the PSD. This approach therefore requires a priori information about how w and m depend on d (n.b. $w(d)$ and $m(d)$ do not necessarily need to be treated separately as per Guidi et al., 2008). For ideal solid objects with constant density, $w \propto d^2$ and $m \propto d^3$ (Kundu et al., 2012), but empirical evidence shows that these scalings are best considered upper bounds that real marine particle populations rarely if ever achieve. The w-d relationship that converts the suspended PSD into the sinking PSD is arguably the more difficult of the two to constrain, either theoretically or empirically, because of the complex dependence of w on various particle properties that are laborious and challenging to measure even for individual particles (Laurenceau-Cornec et al., 2015). However, it is not the w-d relationship particle by particle that matters for the fluxes of biogeochemical and ecological importance, but rather the bulk, statistical relationship between w and d; that is, $w(d)$ is useful as a relationship between the suspended and sinking PSDs.

PSDs in the ocean are most commonly approximated by a power law distribution of the form $n(d) \propto d^{-\xi}$, and in the North Pacific Subtropical Gyre (NPSG), this approximation has been shown to be statistically sound (Barone et al., 2015, Figure 1 and Table 2; White et al., 2015, Figures 1a and 1b) as we also found here (normalized biases of 9–23%; see section 2); see also Andrews et al. (2011), Buonassissi and Dierssen (2010), Kostadinov et al. (2012), and Reynolds et al. (2010). This approximation usefully subsumes the influence of the PSD into a single shape parameter. It also implies that if there is a statistical scaling relationship between d and w—that is, $w \sim d^\alpha$ as readily derived for various idealized cases and commonly used as an ansatz—that $s(d)$ should be power law distributed as well, with

$$s(d) = n\,(d)w(d) \propto d^{-\xi} \times d^\alpha = d_{susp}^{-\xi+\alpha}, \tag{2}$$

which implies that α can be inferred from the difference in ξ for sinking versus suspended PSDs, that is, $\alpha = \xi(n(d)) - \xi(s(d))$. (n.b. If either $n(d)$ or $s(d)$ is not well approximated by a power law, this implies $w \propto d^\alpha$

is a poor approximation of $w(d)$. Also note that while particle (dis)aggregation and consumption affect $s(d)$ and therefore total particle fluxes, this is via affecting $n(d)$.) This can be achieved relatively straightforwardly by capturing particles (e.g., in a sediment trap) and measuring the PSD of the collected material. Furthermore, this gives a collective scaling value for α for the particle population, and thus a $w(d)$ parameterization linking suspended and sinking PSDs, which is difficult to obtain from directly measuring w and d for individual particles without doing so infeasibly many times. Yet to the authors' knowledge, perhaps in part because the sinking PSD is very poorly characterized in the global ocean (and especially in the Pacific) (Durkin et al., 2015; McDonnell & Buesseler, 2010), this method of obtaining an estimate for the size-sinking exponent α has not been attempted to date.

Our objective here is therefore to obtain an estimate for α as the difference in ξ for sinking versus suspended PSDs. Using two optical instruments and a high degree of numerical replication, we measured PSDs for both particles in the water column and those collected in sediment traps. Our study site was Station ALOHA (A Long-term Oligotrophic Habitat Assessment), that of the Hawai'i Ocean Time-series (HOT) program in the NPSG (Karl & Lukas, 1996). While much is known about the magnitude, seasonality, and ecological composition of particle fluxes at Station ALOHA (Boeuf et al., 2019; Emerson et al., 1997; Karl et al., 2012), the characterization of sinking rate-relevant particle characteristics is still somewhat limited, including no reported PSD for sinking material to date to our knowledge. We robustly found an $\alpha \approx 1$, consistent with arguments that marine particles have fractal dimensions of $D \approx 2$ (Alldredge & Gotschalk, 1988; Huang, 1994; Jackson et al., 1995; Jiang & Logan, 1991; Kilps et al., 1994; Li & Logan, 1995; Li et al., 1998; Logan & Wilkinson, 1990; Ploug et al., 2008). This approach to estimating a size-sinking relationship for the total particle population has the potential for wide application and to significantly constrain suspended PSD-based sinking flux estimates.

2. Materials and Methods

All PSD measurements were made in June 2019 at Station ALOHA (22.75°N, 158°W) aboard the R/V *Kilo Moana* (KM1910), using two optical instruments: the Laser In Situ Scatterometer-Transmissometer 100X (Type B, Sequoia Scientific Inc., hereafter LISST) (Agrawal & Pottsmith, 2000) and the Imaging Flow CytoBot (McLane Labs Inc., hereafter IFCB) (Olson & Sosik, 2007). Both instruments have been used extensively both at Station ALOHA (Barone et al., 2015; Dugenne et al., 2020; White et al., 2015) and in many other oceanographic contexts (McDonnell et al., 2015). The LISST uses laser diffraction in an approximately 100 ml sample volume to estimate the PSD via inversion into 32 logarithmically spaced particle size classes. The IFCB images all particles in an approximately 5 ml sample volume that trigger side scatter or chlorophyll fluorescence. Particle volume is then estimated via a distance map algorithm (Moberg & Sosik, 2012). Figure 1 shows an example of the types of data provided by each instrument. Both instruments were used to estimate the PSD of sinking and suspended material for comparison. The image dashboards for all KM1910 IFCB samples can be viewed online (at https://ifcb-data.soest.hawaii.edu/KM1910 and https://ifcb-data.soest.hawaii.edu/KM1910_TRAPS).

Sinking PSDs were measured from material captured in sediment traps. The standard HOT traps and sampling protocol were used (Karl et al., 1996), which includes a 335 μm prefilter to remove zooplankton swimmers. Two sediment trap deployments were sampled: one 81 hr deployment beginning 16 June and one 73 hr deployment beginning 21 June. For each, trap arrays were deployed at 75, 150, and 300 m depths. Each array had 12 traps at each depth. On the second deployment one trap per depth was capped and used as a blank so that there were a total of 69 trap measurements (two deployments and three depths, 11 or 12 traps each). After recovery, from each trap a 125 ml split of the trap solution was taken for LISST and IFCB processing. Sinking PSDs were then measured from the LISST in discrete chamber mode. Twenty diffraction measurements were made from each sample before draining each sample back into the 125 ml split bottle; this process was repeated in triplicate, totaling 60 LISST measurements per sediment trap. Sinking PSDs were then measured from the IFCB by sampling from each trap's split bottle. Trap solution was used as a blank for all LISST measurements.

Suspended PSDs were measured from the LISST by triplicated profile deployments as in White et al. (2015). Suspended PSDs were also measured from discrete bottle samples at the same sample depths and in the same manner as the sediment trap LISST measurements. Particle concentrations in the 300 m discrete suspended

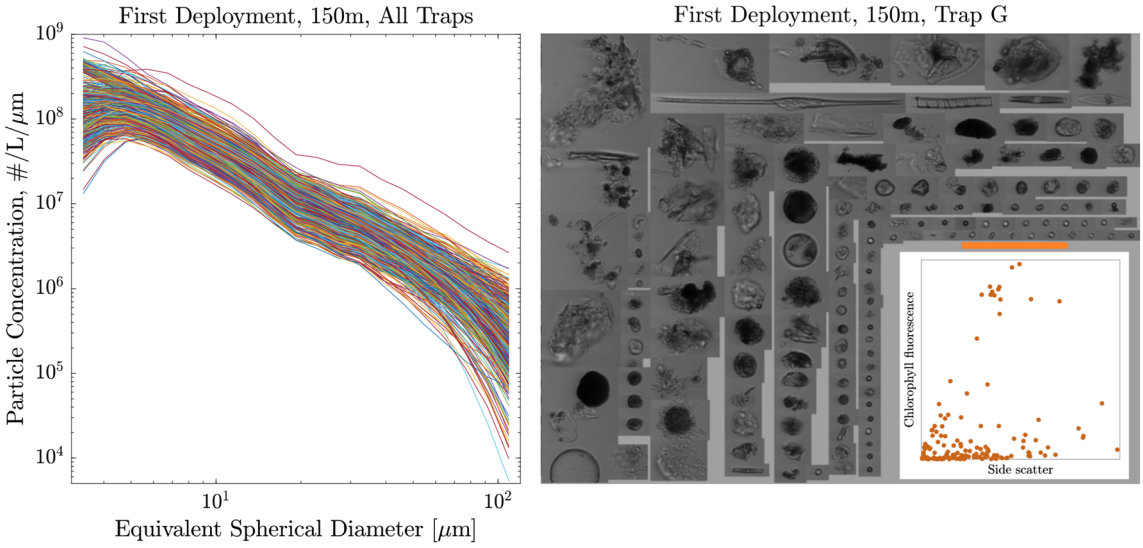

Figure 1. Left: illustration of data collected by the LISST-100X. All PSD measured from the first deployment at 150 m, across 12 sediment traps. Only the size range considered here (3.38–109 μm) is plotted. Right: illustration of data collected by the IFCB. All images taken from a single sediment trap from the first deployment at 150 m ($n = 150$). Inset shows the amplitude of the chlorophyll fluorescence trigger versus the side scatter trigger for the IFCB, indicating that particles vary not only in their size but also in their chlorophyll content. Orange rectangle above the inset is a 100 μm scale bar.

samples were below detection limits and are thus not considered hereafter. Suspended PSDs were measured from the IFCB by sampling continuously from the ship's uncontaminated seawater system, which collects from a nominal 7 m depth. A total of 452 samples were processed by the IFCB in this fashion during the cruise.

The size range we considered in this study was 3.38 to 109 μm; this corresponds to bins 7 to 27 for the LISST and the full size spectrum for the IFCB, which uses a 100 μm mesh prefilter and images particles ~4 μm and larger. The rationale for this selection is as follows: (1) to maximize intercomparability between the two instruments; (2) to maximize comparability with other studies that use similar size ranges (Barone et al., 2015; White et al., 2015); (3) to avoid the effects of density gradients on scattering, which affects bins >100 μm (Barone et al., 2015; Styles, 2006); and (4) because the scattering in the smallest bins for the LISST was in many cases not significantly different (p>0.1 for a one-tailed t test) from that of blanks. The choice of lower/upper bounds has a negligible effect on the results presented here and does not impact our conclusions.

All distributional data were then parameterized by a power law, that is, $p(d) \propto d^{-\xi}$. For the LISST data, which are already PSDs and which we found to be well approximated by a power law distribution for both sinking and suspended particles (all fits were statistically significant with normalized biases of 9–23%; cf. White et al., 2015, and Barone et al., 2015), the exponent was estimated using weighted nonlinear least squares regression as in Barone et al. (2015). Note that the logarithmic spacing of LISST bins must be (and were) accounted for in these analyses. For the IFCB data, which are instead discrete values, this method is not applicable; we instead employed the widely used maximum likelihood approach (Clauset & Newman, 2009; Newman, 2005) and estimated uncertainty in ξ via bootstrapping as in Clauset and Newman (2009). After correction of the raw LISST scattering for either filtered seawater (for discrete suspended samples), 200 m deep water (profiles) or trap solution (sediment samples) blanks, a spherical kernel matrix was applied, and instrument-specific corrections were made using manufacturer supplied code (getscat.m and vdcorr.m) as in White et al. (2015). Particle concentrations below ~145 m in all LISST profiles were too low to yield stable estimates of ξ and are thus not considered hereafter; this is comparable to the 20–150 m range considered by White et al. (2015) except we include data shallower than 20 m as the shallow profile and discrete bottle data are in good agreement, and the winds during KM1910 were calm, likely resulting in a much shallower bubble penetration depth (Vagle et al., 2010) than the annual value used in White et al. (2015). Above 145 m the three profiles were not appreciably different from each other and are therefore treated as replicates.

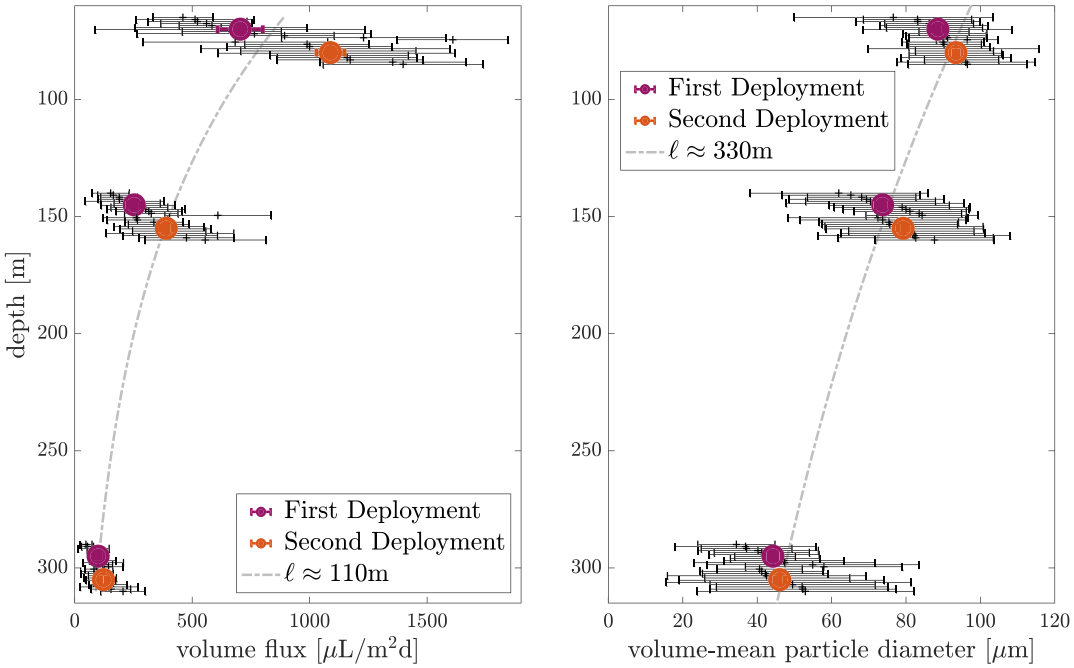

Figure 2. (Left) Volume flux versus depth for both deployments. Black "+" signs are the means for each individual trap, and their error bars are the standard deviations for each individual trap. Purple and orange circles represent the grand mean for each depth and deployment, and their error bars are standard error of the grand mean. Attenuation length scale ℓ is estimated by weighted nonlinear regression. Right: same for volume-weighted mean diameter d_v. In both figures, values are plotted vertically offset for visual aid; all measurements were made from sediment traps deployed at the same three depths (75, 150, and 300 m).

LISST-derived trap PSDs were quality controlled for outliers before further analysis; outliers were almost definitely due to bubbles entrained when pouring the sample into the sample chamber, which cause significant diffraction and are therefore straightforward to detect and to exclude by any reasonable statistical metric. d is computed for IFCB data as the equivalent spherical diameter of a given particles' biovolume, that is, the diameter of a sphere with that same volume. Volume fluxes were calculated from the particle volume concentration, trap solution volume after recovery, the trap collection area, and the deployment time. All discrete suspended and trap samples were handled as gently as possible throughout in order to avoid disruption of particles.

3. Results and Discussion

3.1. Agreement With Historical Data

Before describing our main results, it is useful to note that the data we collected are consistent with historical data for both sinking and suspended material at Station ALOHA. For the sinking material, volume fluxes are within the typical range of HOT carbon fluxes using a standard carbon-to-biovolume conversion factor (Menden-Deuer & Lessard, 2000). We estimate an attenuation length scale of ~110 m from these data (Figure 2) via weighted nonlinear least squares regression, which is also within the range of mass flux-based attenuation length-scale data for Station ALOHA. IFCB-based abundances from the underway system at ~7 m were within typical ranges although we observed comparatively high abundances of filaments of the large nitrogen-fixing *Trichodesmium spp*. Suspended PSD ξ values and mean diameters d_a (see below) were within typical ranges as well (White et al., 2015), though ξ values were on the lower end of this range, likely due to the aforementioned *Trichodesmium* bloom. We must acknowledge that the PSD slope of sinking particles may be influenced by potential aggregation/disaggregation during sample processing. However, gel trap collections at Station ALOHA indicate a PSD slope of 1.8–2.0 (Nelson et al., 2018), generally consistent with our measured sinking PSD (2.0–2.3). The small offset of these measurements may reflect temporal differences in the PSD of settling particles, underestimation of <10 μm particles via gel traps (Durkin et al., 2015), or indicate that our data are slightly biased toward small particles either via

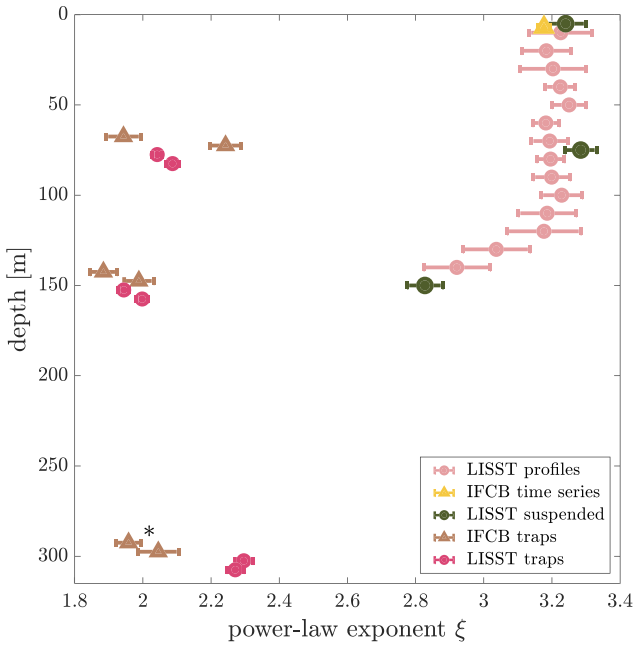

Figure 3. PSD exponent ξ of sinking and suspended material for different depths, deployments, and instruments. Error bars in all cases are standard error of the grand mean. Trap-derived ξ values are plotted vertically offset for visual aid; all measurements were made from sediment traps deployed at the same three depths (75, 150, and 300 m). *We have low confidence in the IFCB-derived ξ values at 300 m as these are based on small sample sizes, ≤10 particles/ml.

underestimation of rare, large particles or net particle disaggregation during handling. Furthermore, we observed good agreement in all measured parameters between instruments, sediment trap deployments, and between discrete and profiling LISST samples. The exception to this is the sediment traps at 300 m, where the IFCB data yield lower ξ values than the LISST data; however, this may be an artifact of the small sample size at this depth ($n \leq 10$ particles/ml).

3.2. Linear Scaling of Sinking Speed With Size

Figure 3 summarizes our main findings. For material suspended in the water column, the PSD has a relatively steady exponent of $\xi \approx 3.2$ from the shallowest depths to ~125 m and then appears to decrease to a value closer to $\xi \approx 2.8$ from 125–150 m. In contrast, the PSD of sinking material is much lower, with $\xi \approx 2$–2.3 across all depths sampled. This implies a $w \sim d^{\alpha}$ scaling of roughly $\alpha \approx 1$, though the exact α value depends of course on which data ξ is defined from for sinking and suspended PSDs. Across all plausible combinations from the values in Figure 3, α is within the range 1.05 ± 0.2. This approximately linear sinking speed-diameter scaling is far from the frequently utilized value of $\alpha = 2$ for ideal solid constant-density spheres.

This $\alpha \approx 1$ scaling is instead more consistent with a fractal description of marine particles; a fractal particle of dimension D will exhibit a scaling of $\alpha = D - 1$ (Jackson, 1995), here implying a fractal dimension of $D \approx 2$. The fractal dimension of marine particles has been an object of study for decades, and while there is undoubtedly both ecological and methodological variation in D, a substantial body of evidence suggests that marine particles have a fractal dimension of $D \approx 2$ rather than $D \approx 3$ (albeit with significant variability between methods, definitions, and samples) (Alldredge & Gotschalk, 1988; Huang, 1994; Jackson et al., 1995; Jiang & Logan, 1991; Kilps et al., 1994; Li & Logan, 1995; Li et al., 1998; Logan & Wilkinson, 1990; Ploug et al., 2008). This also includes the suspended PSD versus mass flux comparison by Guidi et al. (2008), which found $b = 3.52$, wherein b is the sum of both α and a mass-to-diameter scaling it should equal $2D - 1$, implying $D = 2.26$. Thus, $\alpha \approx 1$ as we find here is consistent with these studies. A lower α (and/or D) than 2 (3) also implies a relatively more important role for smaller particles in total sinking fluxes, as has been increasingly recognized (Alonso-González et al., 2010; Durkin et al., 2015; Riley et al., 2012).

One can also estimate sinking velocities for an individual size class by dividing the flux in that size class by the ambient concentration in that size class (McDonnell & Buesseler, 2010). Results from this approach were in good agreement (≤25%, median 15%) with the power law approximation, except for the largest size bin, where the power law approximation overestimated settling velocities by ~50%. Thus, it appears that the largest size (93–109 μm) bin's velocities may have been overestimated here (though note that as the LISST estimates the entire size distribution via regularized inversion, it is not ideally suited to estimating properties of individual size bins and therefore to the application of the McDonnell & Buesseler, 2010, approach). Nonetheless, our main conclusions are not affected by this discrepancy.

3.3. Mean Diameters

Though the power law exponent ξ is a more useful and easily estimated quantity than the moments of a power law distribution (Newman, 2005), it is still instructive to consider the distributions' means. Table 1 shows various mean diameters from the LISST-derived sinking PSDs. d_n is the arithmetic mean, d_a is the area-weighted mean, and d_v is the volume-weighted mean. As usual for power law distributed data, d_n is close to $\min(d)$. d_a when compared with historical LISST water column data for Station ALOHA (with which the profiles described here are consistent) shows that as expected, larger particles are comparatively more responsible for sinking fluxes. An arguably better metric for this is d_v, which corresponds to the expected value of the diameter of a particle containing a randomly chosen parcel of particle volume. We estimate

Table 1
Mean Diameters d (μm) for Different Definitions, Depths, and Deployments

	d_v	d_a	d_n
75 m	88.6 (1.6) | 93.4 (0.6)	40.7 (0.8) | 35.2 (0.8)	7.44 (0.07) | 7.05 (0.10)
150 m	73.7 (1.9) | 79.2 (1.3)	37.0 (1.7) | 36.0 (0.8)	7.94 (0.14) | 7.54 (0.04)
300 m	44.2 (2.3) | 46.1 (1.3)	20.9 (1.3) | 19.8 (0.6)	6.96 (0.12) | 6.87 (0.05)

Note. Subscripts *v*, *a*, and *n* refer to volume, area, and number weighted. Number on the left (right) in each cell refers to the first (second) deployment. Number in parentheses refers to standard error of the grand mean.

by weighted nonlinear least squares regression the attenuation length scale of d_v to be ~330 m, that is, three times that of volume flux, as expected because equivalent spherical diameter by definition scales as volume to the 1/3 power. The consistency between these length scales suggests that the attenuation of volume flux with depth is due to particles becoming smaller rather than fewer in number (Figure 2). Most notably, the relatively small mean diameter values in Table 1 evince the importance of small particles to the total flux. For comparison in situ pump-based flux studies (e.g., Pavia et al., 2019) typically use a cutoff of 51 μm to define "small" and "large" particles. Our results therefore further underscore the relative importance of small particle fluxes, at least in the NPSG.

For a true power law, the mean is given by $d_n = \frac{\xi - 1}{\xi - 2}\min(d)$ (Newman, 2005), meaning that as $\xi \approx 2$ for the trap data, the IFCB cannot be used to provide reliable estimates of any of these mean diameters for sinking PSDs (the median IFCB-derived ξ value across all 69 traps is 2.01 ± 0.14). The LISST on the other hand estimates the entire PSD over a finite interval and therefore can reliably be used to estimate means. In contrast, for the continuous data from ~7 m where $\xi = 3.18 \pm 0.02$, IFCB-derived d_n,d_a, and d_v agree well with the LISST-derived values and estimates derived from (ξ, min(d)).

3.4. Conclusion

To summarize, we have shown that by comparing the PSDs of sinking and suspended material, one can infer a bulk relationship between size and sinking speed. We found at Station ALOHA that this relationship is approximately linear, which is more consistent with particles being fractal like than sphere like. We found this relationship to be robust in several respects. Our results are the first to our knowledge to characterize the sinking PSD at Station ALOHA or in the NPSG. Our results indicate that at Station ALOHA sediment trap-derived particle fluxes are dominated by relatively small particles, that is, particles less than the 53 μm cutoff used in in situ pump studies and that these "small" particles are increasingly important with depth due to disaggregation and microbial consumption (Collins et al., 2015).

Here we have focused on particles ~100 μm or less in diameter in part because our measurements detected few particles outside of this range. In less oligotrophic systems, larger particles are thought to contribute appreciably to the total flux (Fowler & Knauer, 1986). The approach we have developed here is equally applicable to these systems and particle sizes (though we note that other instruments would have to be used to measure particles hundreds of microns in diameter, and if either the sinking or suspended PSD were not well approximated by a power law distribution, this would imply a $w(d)$ relationship different from a power law scaling); in future studies it would be instructive to compare the relationship between sinking and suspended PSDs (and the inferred size-sinking relationship) for other ecosystems and size ranges. As this approach uses technologies that are relatively common in oceanographic settings and permits a large degree of replication, we believe it has the potential to be applied widely and can aid in constraining PSD-based estimates of sinking fluxes in the ocean, especially if paired with size-fractionated stoichiometric measurements. Such parameterizations are becoming increasingly invaluable for the study of the biological pump with the rising prevalence of integrated optical sensor packages.

Data Availability Statement

All IFCB data are available online (at https://ifcb-data.soest.hawaii.edu/KM1910), and code and LISST data are provided at Zenodo and GitHub (https://zenodo.org/record/3816721\#.Xvx_h5NKgp8and https://github.com/bbcael).

Acknowledgments

This work was funded by a Life Sciences-Simons Postdoctoral Fellowship in Marine Microbial Ecology (Award 602351, B. B. C.), the Simons Foundation SCOPE program (Award P49800, A. W.), and the National Science Foundation (Award 1911990, A. W.). The authors are grateful to Matthew Church, Erica Goetze, Sara Ferrón, Mathilde Dugenne, Tara Clemente, David M. Karl, and all of those involved with the NSF EAGER cruise KM1910 for providing the opportunity to make the necessary measurements for this work, including accommodating our request to sample from every single sediment trap. David M. Karl also provided useful comments on a draft manuscript.

References

Agrawal, Y. C., & Pottsmith, H. C. (2000). Instruments for particle size and settling velocity observations in sediment transport. *Marine Geology*, *168*(1-4), 89–114.

Alldredge, A. L., & Gotschalk, C. (1988). In situ settling behavior of marine snow. *Limnology and Oceanography*, *33*(3), 339–351.

Alonso-González, I. J., Arístegui, J., Lee, C., Sanchez-Vidal, A., Calafat, A., Fabrés, J., et al. (2010). Role of slowly settling particles in the ocean carbon cycle. *Geophysical Research Letters*, *37*, L13608. https://doi.org/10.1029/2010GL043827

Andrews, S. W., Nover, D. M., Reuter, J. E., & Schladow, S. G. (2011). Limitations of laser diffraction for measuring fine particles in oligotrophic systems: Pitfalls and potential solutions. *Water Resources Research*, *47*, W05523. https://doi.org/10.1029/2010WR009837

Barone, B., Bidigare, R. R., Church, M. J., Karl, D. M., Letelier, R. M., & White, A. E. (2015). Particle distributions and dynamics in the euphotic zone of the North Pacific Subtropical Gyre. *Journal of Geophysical Research: Oceans*, *120*, 3229–3247. https://doi.org/10.1002/2015JC010774

Berger, W. H. (1971). Sedimentation of planktonic foraminifera. *Marine Geology*, *11*(5), 325–358.

Boeuf, D., Edwards, B. R., Eppley, J. M., Hu, S. K., Poff, K. E., Romano, A. E., et al. (2019). Biological composition and microbial dynamics of sinking particulate organic matter at abyssal depths in the oligotrophic open ocean. *Proceedings of the National Academy of Sciences*, *116*(24), 11,824–11,832.

Buesseler, K. O., Antia, A. N., Chen, M., Fowler, S. W., Gardner, W. D., Gustafsson, O., et al. (2007). An assessment of the use of sediment traps for estimating upper ocean particle fluxes. *Journal of Marine Research*, *65*(3), 345–416.

Buonassissi, C. J., & Dierssen, H. M. (2010). A regional comparison of particle size distributions and the power law approximation in oceanic and estuarine surface waters. *Journal of Geophysical Research*, *115*, C10028. https://doi.org/10.1029/2010JC006256

Burd, A. B., & Jackson, G. A. (2009). Particle aggregation. *Annual Review of Marine Science*, *1*, 65–90.

Chisholm, S. W. (1992). Phytoplankton size, *Primary productivity and biogeochemical cycles in the sea* (pp. 213–237). Boston, MA: Springer.

Clauset, S. C. R., & Newman, M. E. J. (2009). Power-law distributions in empirical data. *SIAM Review*, *51*(4), 661–703.

Collins, J. R., Edwards, B. R., Thamatrakoln, K., Ossolinski, J. E., DiTullio, G. R., Bidle, K. D., et al. (2015). The multiple fates of sinking particles in the North Atlantic Ocean. *Global Biogeochemical Cycles*, *29*, 1471–1494. https://doi.org/10.1002/2014GB005037

DeVries, T., Primeau, F., & Deutsch, C. (2012). The sequestration efficiency of the biological pump. *Geophysical Research Letters*, *39*, L13601. https://doi.org/10.1029/2012GL051963

Dugenne, M., HendrikxFreitas, F., Wilson, S. T., Barone, B., Karl, D. M., & White, A. E. (2020). Life and death of Crocosphaera sp. in the Pacific Ocean: Fine scale predator-prey dynamics. *Limnology and Oceanography*. https://doi.org/10.1002/lno.11473

Durkin, C. A., Estapa, M. L., & Buesseler, K. O. (2015). Observations of carbon export by small sinking particles in the upper mesopelagic. *Marine Chemistry*, *175*, 72–81.

Emerson, S., Quay, P., Karl, D., Winn, C., Tupas, L., & Landry, M. (1997). Experimental determination of the organic carbon flux from open-ocean surface waters. *Nature*, *389*(6654), 951.

Fowler, S. W., & Knauer, G. A. (1986). Role of large particles in the transport of elements and organic compounds through the oceanic water column. *Progress in oceanography*, *16*(3), 147–194.

Gardner, W. D. (2000). Sediment trap sampling in surface waters. In R. B. Hanson, H. W. Ducklow & J. G. Field (Eds.), *The Changing Ocean Carbon Cycle: A Mid-term Synthesis of the Joint Global Ocean Flux Study* (pp. 240–281). Cambridge: Cambridge University Press.

Guidi, L., Jackson, G. A., Stemmann, L., Miquel, J. C., Picheral, M., & Gorsky, G. (2008). Relationship between particle size distribution and flux in the mesopelagic zone. *Deep Sea Research Part I: Oceanographic Research Papers*, *55*(10), 1364–1374.

Honjo, S., Connell, J. F., & Sachs, P. L. (1980). Deep-ocean sediment trap; design and function of PARFLUX Mark II. *Deep Sea Research Part A. Oceanographic Research Papers*, *27*(9), 745–753.

Huang, H. (1994). Fractal properties of flocs formed by fluid shear and differential settling. *Physics of Fluids*, *6*(10), 3229–3234.

Jackson, G. (1995). Comparing observed changes in particle size spectra with those predicted using coagulation theory. *Deep Sea Research Part II: Topical Studies in Oceanography*, *42*, 159–184.

Jackson, G. A., Logan, B. E., Alldredge, A. L., & Dam, H. G. (1995). Combining particle size spectra from a mesocosm experiment measured using photographic and aperture impedance (Coulter and Elzone) techniques. *Deep Sea Research Part II: Topical Studies in Oceanography*, *42*(1), 139–157.

Jiang, Q., & Logan, B. E. (1991). Fractal dimensions of aggregates determined from steady-state size distributions. *Environmental Science & Technology*, *25*(12), 2031–2038.

Jouandet, M.-P., Trull, T. W., Guidi, L., Picheral, M., Ebersbach, F., Stemmann, L., & Blain, S. (2011). Optical imaging of mesopelagic particles indicates deep carbon flux beneath a natural iron-fertilized bloom in the southern ocean. *Limnology and Oceanography*, *56*(3), 1130–1140.

Karl, D. M., Christian, J. R., Dore, J. E., Hebel, D. V., Letelier, R. M., Tupas, L. M., & Winn, C. D. (1996). Seasonal and interannual variability in primary production and particle flux at station ALOHA. *Deep Sea Research Part II: Topical Studies in Oceanography*, *43*(2-3), 539–568.

Karl, D. M., Church, M. J., Dore, J. E., Letelier, R. M., & Mahaffey, C. (2012). Predictable and efficient carbon sequestration in the North Pacific Ocean supported by symbiotic nitrogen fixation. *Proceedings of the National Academy of Sciences*, *109*(6), 1842–1849.

Karl, D. M., & Lukas, R. (1996). The Hawaii Ocean Time-series (HOT) program: Background, rationale and field implementation. *Deep Sea Research Part II: Topical Studies in Oceanography*, *43*(2-3), 129–156.

Kilps, J. R., Logan, B. E., & Alldredge, A. L. (1994). Fractal dimensions of marine snow determined from image analysis of in situ photographs. *Deep Sea Research Part I: Oceanographic Research Papers*, *41*(8), 1159–1169.

Kostadinov, T. S., Siegel, D. A., Maritorena, S., & Guillocheau, N. (2012). Optical assessment of particle size and composition in the Santa Barbara Channel, California. *Applied optics*, *51*(16), 3171–3189.

Kundu, P. K., Cohen, I. M., & Dowling, D. R. (Eds.). (2012). *Fluid mechanics* (5th Ed.). Hoboken, NJ: Academic Press. ISBN 9780123821003. https://doi.org/10.1016/B978-0-12-382100-3.10004-6

Laurenceau-Cornec, E. C., Trull, T. W., Davies, D. M., Christina, L., & Blain, S. (2015). Phytoplankton morphology controls on marine snow sinking velocity. *Marine Ecology Progress Series*, *520*, 35–56.

Li, X., & Logan, B. E. (1995). Size distributions and fractal properties of particles during a simulated phytoplankton bloom in a mesocosm. *Deep Sea Research Part II: Topical Studies in Oceanography*, *42*(1), 125–138.

Li, X., Passow, U., & Logan, B. E. (1998). Fractal dimensions of small (15–200 μm) particles in Eastern Pacific coastal waters. *Deep Sea Research Part I: Oceanographic Research Papers*, *45*(1), 115–131.

Logan, B. E., & Wilkinson, D. B. (1990). Fractal geometry of marine snow and other biological aggregates. *Limnology and Oceanography*, *35*(1), 130–136.
McDonnell, A. M. P., & Buesseler, K. O. (2010). Variability in the average sinking velocity of marine particles. *Limnology and Oceanography*, *55*(5), 2085–2096.
McDonnell, A. M. P., Lam, P. J., Lamborg, C. H., Buesseler, K. O., Sanders, R., Riley, J. S., et al. (2015). The oceanographic toolbox for the collection of sinking and suspended marine particles. *Progress in oceanography*, *133*, 17–31.
Menden-Deuer, S., & Lessard, E. J. (2000). Carbon to volume relationships for dinoflagellates, diatoms, and other protist plankton. *Limnology and oceanography*, *45*(3), 569–579.
Moberg, E. A., & Sosik, H. M. (2012). Distance maps to estimate cell volume from two-dimensional plankton images. *Limnology and Oceanography: Methods*, *10*(4), 278–288.
Nelson, A. J., Church, M. J., Dornan, N., Kyi, E., Van Mooy, B., Ossolinski, J., & Viviani, D. (2018). Poster 29138: Rates of microbial activities associated with sinking particles at Station ALOHA in the North Pacific Subtropical Gyre. Ocean Sciences Meeting 2018, Portland, Oregon, USA.
Newman, M. E. J. (2005). Power laws, Pareto distributions and Zipf's law. *Contemporary Physics*, *46*(5), 323–351.
Olson, R. J., & Sosik, H. M. (2007). A submersible imaging-in-flow instrument to analyze nano- and microplankton: Imaging Flowcytobot. *Limnology and Oceanography: Methods*, *5*(6), 195–203.
Pavia, F. J., Anderson, R. F., Lam, P. J., Cael, B. B., Vivancos, S. M., Fleisher, M. Q., et al. (2019). Shallow particulate organic carbon regeneration in the South Pacific Ocean. *Proceedings of the National Academy of Sciences*, *116*(20), 9753–9758.
Ploug, H., Iversen, M. H., & Fischer, G. (2008). Ballast, sinking velocity, and apparent diffusivity within marine snow and zooplankton fecal pellets: Implications for substrate turnover by attached bacteria. *Limnology and Oceanography*, *53*(5), 1878–1886.
Reynolds, R. A., Stramski, D., Wright, V. M., & Woźniak, S. B. (2010). Measurements and characterization of particle size distributions in coastal waters. *Journal of Geophysical Research: Oceans*, *115*, C08024. https://doi.org/10.1029/2009JC005930
Riley, J. S., Sanders, R., Marsay, C., LeMoigne, F. A. C., Achterberg, E. P., & Poulton, A. J. (2012). The relative contribution of fast and slow sinking particles to ocean carbon export. *Global Biogeochemical Cycles*, *26*, GB1026. https://doi.org/10.1029/2011GB004085
Smayda, T. J. (1970). The suspension and sinking of phytoplankton in the sea. *Oceanography and Marine Biology - An Annual*, *8*, 353–414.
Styles, R. (2006). Laboratory evaluation of the LISST in a stratified fluid. *Marine Geology*, *227*(1-2), 151–162.
Trull, T. W., Bray, S. G., Buesseler, K. O., Lamborg, C. H., Manganini, S., Moy, C., & Valdes, J. (2008). In situ measurement of mesopelagic particle sinking rates and the control of carbon transfer to the ocean interior during the Vertical Flux in the Global Ocean (VERTIGO) voyages in the North Pacific. *Deep Sea Research Part II: Topical Studies in Oceanography*, *55*(14-15), 1684–1695.
Vagle, S., McNeil, C., & Steiner, N. (2010). Upper ocean bubble measurements from the NE Pacific and estimates of their role in air-sea gas transfer of the weakly soluble gases nitrogen and oxygen. *Journal of Geophysical Research*, *115*, C12054. https://doi.org/10.1029/2009JC005990
White, A. E., Letelier, R. M., Whitmire, A. L., Barone, B., Bidigare, R. R., Church, M. J., & Karl, D. M. (2015). Phenology of particle size distributions and primary productivity in the North Pacific subtropical gyre (Station ALOHA). *Journal of Geophysical Research: Oceans*, *120*, 7381–7399. https://doi.org/10.1002/2015JC010897